Competition between 1,2-Diol and 2-Hydroxy Acid Coordination in Cr(V)-Quinic Acid Complexes: Implications for Stabilization of Cr(V) Intermediates of Relevance to Cr(VI)-Induced Carcinogenesis

Rachel Codd and Peter A. Lay*

Contribution from the School of Chemistry, University of Sydney, New South Wales 2006, Australia
Received March 25, 1999

Abstract: For the speciation of Cr(V) intermediates formed during the intracellular reduction of Cr(VI) to be understood, the intramolecular competition between 1,2-diol and 2-hydroxy acid coordination to Cr(V) as a function of pH has been studied in quinic acid complexes. The Cr(V)-2-hydroxy acid complex, K[Cr(O)-$(qaH_3)_2]\cdot H_2O$ (qaH_5 = 1*R*,3*R*,4*R*,5*R*-1,3,4,5-tetrahydroxycyclohexanecarboxylic acid, **I**), has been isolated and characterized. In aqueous solutions at pH values <4.0, $K[Cr(O)(qaH_3)_2]\cdot H_2O$ gives two EPR signals (g_{iso} = 1.9787, $A_{iso} = 17.2 \times 10^{-4}$ cm^{-1}; g_{iso} = 1.9791, $A_{iso} = 16.4 \times 10^{-4}$ cm^{-1}). The relative intensities of the signals are independent of $[qaH_5]/[Cr(V)]$, and of increasing $[qaH_5]$ and [Cr(V)] at constant $[qaH_5]/[Cr(V)]$ and pH values. These signals are consistent with those found with well-characterized Cr(V)-2-hydroxy acid complexes and are assigned to two geometric isomers of the $[Cr(O)(O^1,O^7\text{-}qaH_3)_2]^-$ linkage isomer. Both the 2-hydroxy acid (O^1,O^7) and *vic*-diol (cis-O^3,O^4; trans-O^4,O^5) groups of qaH_5 are viable Cr(V) donors. In the reduction of Cr(VI) by GSH in the presence of an excess of qaH_5, the EPR spectra are similar to that of $K[Cr(O)(qaH_3)_2]\cdot H_2O$ at low pH values (<4.0). At intermediate pH values (pH 5−7.5) additional signals appear (g_{iso} = 1.9791, g_{iso} = 1.9794, g_{iso} = 1.9799), which have EPR spectral data consistent with the presence of Cr(V)-qa linkage isomers, featuring one of each donor type (1 × 2-hydroxy acid; 1 × diol). By using EPR spectral simulation, we deduced that the *cis*-diol linkage isomer, $[Cr(O)(O^1,O^7\text{-}qaH_3)(O^3,O^4\text{-}qaH_2)]^{2-}$, is an order of magnitude more thermodynamically stable to intramolecular ligand exchange compared to the *trans*-diol linkage isomer, $[Cr(O)(O^1,O^7\text{-}qaH_3)(O^4,O^5\text{-}qaH_2)]^{2-}$. At pH values >7.5, the Cr(V)-qa EPR spectra reveal two triplets (g_{iso} = 1.9800, g_{iso} = 1.9802), which are ascribed to geometric isomers of a bis-diol Cr(V)-qa complex, $[Cr(O)(O^3,O^4\text{-}qaH_2)_2]^{3-}$. The concentration of the *trans*-diol isomer, $[Cr(O)(O^4,O^5\text{-}qaH_2)_2]^{3-}$, is predicted to be negligible. This assignment is supported by the similarity of the EPR spectral data with those formed in the Cr(VI) reduction by GSH in the presence of the related polyol (cis-O^3,O^4; trans-O^4,O^5) ligand, shikimic acid (3*R*,4*R*,5*R*-3,4,5-trihydroxycyclohexenecarboxylic acid, **II**), which does not possess a 2-hydroxy acid moiety. The relative intensities of the EPR signals of the Cr(V)-sa species (g_{iso} = 1.9800, g_{iso} = 1.9801), ascribed to geometric isomers of $[Cr(O)(O^3,O^4\text{-}saH)_2]^{3-}$, are independent of increasing pH and of $[saH_4]$ at pH values >4.0. The results show that 2-hydroxy acid ligands are favored with respect to 1,2-diols for stabilizing Cr(V) at low pH values relevant to phagocytosis of insoluble chromates (pH ∼4), but the opposite is the case when soluble chromates are taken up by the cells at pH = 7.4. Both classes of ligands compete effectively for complexation of Cr(V) compared to glutathione at all pH values studied.

Introduction

Occupational exposure to Cr(VI) in industries such as stainless steel welding and electroplating[1] is of great concern, due to its known carcinogenicity toward humans.[2] While it is undisputed that Cr(VI) is carcinogenic,[2] there exists a healthy debate regarding the species most likely to be responsible for cellular damage and the mechanism(s) involved in genotoxic damage.[3−5] Chromium(VI) itself is unable to react with DNA in vitro[4,6,7] or with isolated nuclei,[8,9] but in the presence of reducing agents, it causes a wide variety of DNA lesions, including Cr-DNA adducts,[6,10−13] DNA−DNA cross-links,[14,15] DNA−protein cross-links,[7,9,16] apyrimidinic/apurinic (AP) sites,[17−20] and oxidative

(1) Yassi, A.; Nieboer, E. In *Chromium in the Natural and Human Environments*; Nriagu, J. O., Nieboer, E., Eds.; Wiley-Interscience: New York, 1988; pp 443−495.

(2) *IARC Monographs on the Evaluation of the Carcinogenic Risk of Chemicals to Humans*; International Agency for Research on Cancer: Lyon, France, 1990; Vol. 49, pp 127−198.

(3) Standeven, A. M.; Wetterhahn, K. E. *Chem. Res. Toxicol.* **1991**, *4*, 616−625.

(4) Farrell, R. P.; Judd, R. J.; Lay, P. A.; Dixon, N. E.; Baker, R. S. U.; Bonin, A. M. *Chem. Res. Toxicol.* **1989**, *2*, 227−229.

(5) Shi, X.; Mao, Y.; Knapton, A. D.; Ding, M.; Rojanasakul, Y.; Gannett, P. M.; Dalal, N.; Liu, K. *Carcinogenesis* **1994**, *15*, 2475−2478.

(6) Tsapakos, M. J.; Wetterhahn, K. E. *Chem.-Biol. Interact.* **1983**, *46*, 265−277.

(7) Fornace, J., A. J.; Seres, D. S.; Lechner, J. F.; Harris, C. C. *Chem-Biol. Interact.* **1981**, *36*, 345−354.

(8) Bianchi, V.; Levis, A. G. In *Carcinogenic and Mutagenic Metal Compounds*; Merian, E., Frei, R. W., Härdi, W., Schlatter, C., Eds.; Gordon and Breach Science Publishers: London, U.K., 1985; pp 269−293.

(9) Miller, C. A., III; Cohen, M. D.; Costa, M. *Carcinogenesis* **1991**, *12*, 269−276.

(10) Borges, K. M.; Boswell, J. S.; Liebross, R. H.; Wetterhahn, K. E. *Carcinogenesis* **1991**, *12*, 551−561.

(11) Aiyar, J.; Borges, K. M.; Floyd, R. A.; Wetterhahn, K. E. *Toxicol. Environ. Chem.* **1989**, *22*, 135−148.

(12) Borges, K. M.; Wetterhahn, K. E. *Carcinogenesis* **1989**, *10*, 2165−2168.

(13) Hneihen, A. S.; Standeven, A. M.; Wetterhahn, K. E. *Carcinogenesis* **1993**, *14*, 1795−1803.

(14) De Flora, S.; Wetterhahn, K. E. *Life Chem. Rep.* **1989**, *7*, 169−244.

(15) Bianchi, V.; Celotti, L.; Lanfranchi, G.; Majone, F.; Marin, G.; Montaldi, A.; Sponza, G.; Tamino, G.; Venier, P.; Zantedeschi, A.; Levis, A. G. *Mutat. Res.* **1983**, *117*, 279−300.

10.1021/ja9909780 CCC: $18.00
Published on Web 08/12/1999

damage.[21] Selected genotoxic effects of Cr(VI) observed in vivo include chromosomal aberrations and the formation of micronuclei, sister-chromatid exchanges, DNA strand breaks, and unscheduled DNA synthesis.[22] Following the discovery of a long-lived EPR-active Cr(V) species, formed upon the reduction of Cr(VI) by microsomes in the presence of NADPH,[23] attention became focused on the possible role(s) played by Cr(V) species in Cr(VI)-induced carcinogenesis. This led to the formation of the uptake-reduction model of Cr(VI)-induced carcinogenesis, which postulates that Cr(VI) enters the cell via the nonspecific anion-transport channels and is then reduced intracellularly, yielding species that are reactive toward genetic material.[24] The reactive intermediates implicated include the following: Cr(VI) esters, Cr(V) or Cr(IV) species, and radical species (hydroxyl and thiyl).[24] Chromium(VI) may be reduced enzymatically[25] or by small molecular weight redox-active molecules, such as ascorbate,[24] glutathione (GSH),[26] hydroxy acids, or nucleotides.[26,27]

Extensive studies on the readily synthesized,[28,29] relatively stable Cr(V)-2-hydroxy acid complexes, $[Cr(O)(ehba)_2]^-$ (ehba = 2-ethyl-2-hydroxybutanoato(2−)) and $[Cr(O)(hmba)_2]^-$ (hmba = 2-hydroxy-2-methylbutanoato(2−)),[30−32] have illustrated that $[Cr(O)(ehba)_2]^-$ induces cleavage of negatively supercoiled plasmid DNA (pUC9)[4,32] and is mutagenic with V79 Chinese hamster lung cells in the micronucleus assay.[33] The Cr(V)-2-hydroxy acid complexes are useful models for understanding the chemistry in vivo between Cr(V) and naturally occurring intracellular 2-hydroxy acids, such as, lactic and citric acids, and the oxidized forms of sugars (aldonic, aldaric, and uronic acids).

Several studies have also examined Cr(V)-diol speciation,[34−39] which is important because Cr(V) species are formed by the Cr(VI) oxidation of ribonucleotides but not deoxyribonucleotides,[27] suggesting that the *cis*-diol group of the ribonucleotide is involved in coordination. A recent study used EPR spectroscopy to examine the metabolism of Cr(VI) in rats and assigned the EPR signal to a Cr(V)-diol species formed with NADP,[40] which was consistent with the results from in vitro experiments involving the reduction of Cr(VI) by NADPH and microsomes.[23] The definitive assignment of the species as a Cr(V)-NADP species, however, is questionable, on the basis of similar g_{iso} and ^1H a_{iso} values observed in EPR spectra formed upon the reduction of Cr(VI) by GSH, in the presence of D-glucose.[37,41] More recently, the species formed between Cr(V) and *cis*- and *trans*-1,2-cyclohexanediol have been examined using EPR spectroscopy, in an attempt to better understand the species formed between Cr(V) and D-glucose.[37] Because of their potential biological relevance, Cr(V)-sugar complexes have been the focus of several studies and have been characterized by electrochemistry[42,43] and EPR[39,41,44−47] and electronic absorption spectroscopies.[42] The effect upon Cr(V) speciation of different intracellular pH values present in phagocytic cells has yet to be thoroughly investigated. The Cr(V) species formed at normal physiological pH values (pH ∼7.4) are likely to be significantly different from those formed at lower (or higher) pH values. The study of Cr(V) speciation at low pH values has relevance with respect to phagocytosis of insoluble chromates, where the pH of the vacuole becomes more acidic (pH ∼4−5).[48]

The naturally occurring *tert*-2-hydroxy acid, quinic acid (**I**, 1*R*,3*R*,4*R*,5*R*-1,3,4,5-tetrahydroxycyclohexanecarboxylic acid, qaH_5) is an ideal ligand to study the effect of pH upon Cr(V)

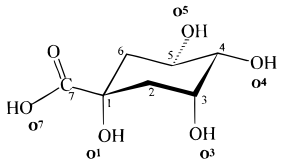

I

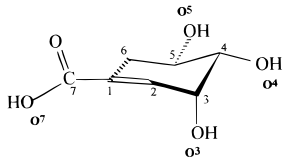

II

speciation with biologically relevant donor groups. The polyhydroxy-substituted cyclohexane ring well represents carbohydrates and inositols. Other functional groups ubiquitous in nature

(16) Xu, J.; Manning, F. C. R.; Patierno, S. R. *Carcinogenesis* **1994**, *15*, 1443−1450.
(17) Casadevall, M.; Kortenkamp, A. *Carcinogenesis* **1995**, *16*, 805−809.
(18) Casadevall, M.; Kortenkamp, A. *Carcinogenesis* **1994**, *15*, 407−409.
(19) da Cruz Fresco, P.; Shacker, F.; Kortenkamp, A. *Chem. Res. Toxicol.* **1995**, *8*, 884−890.
(20) Kortenkamp, A.; Casadevall, M.; da Cruz Fresco, P. *Ann. Clin. Lab. Sci.* **1996**, *26*, 160−175.
(21) Cohen, M. D.; Kargacin, B.; Klein, C. B.; Costa, M. *Crit. Rev. Toxicol.* **1993**, *23*, 255−281.
(22) Nieboer, E.; Shaw, S. L. In *Chromium in the Natural and Human Environments*; Nriagu, J. O., Nierboer, E., Eds.; Wiley-Interscience: New York, 1988; pp 399−441.
(23) Wetterhahn Jennette, K. *J. Am. Chem. Soc.* **1982**, *104*, 874−875.
(24) Connett, P. H.; Wetterhahn, K. E. *Struct. Bonding (Berlin)* **1983**, *54*, 93−124.
(25) Garcia, J. D.; Wetterhahn Jennette, K. *J. Inorg. Biochem.* **1981**, *14*, 281−295.
(26) Connett, P. H.; Wetterhahn, K. E. *J. Am. Chem. Soc.* **1985**, *107*, 4282−4288.
(27) Goodgame, D. M. L.; Hayman, P. B.; Hathway, D. E. *Polyhedron* **1982**, *1*, 497−499.
(28) Krumpolc, M.; DeBoer, B. G.; Roček, J. *J. Am. Chem. Soc.* **1978**, *100*, 145−153.
(29) Krumpolc, M.; Roček, J. *J. Am. Chem. Soc.* **1979**, *101*, 3206−3209.
(30) Codd, R., Ph.D. Thesis, The University of Sydney, 1997.
(31) Sugden, K. D.; Wetterhahn, K. E. *Chem. Res. Toxicol.* **1997**, *10*, 1397−1405.
(32) Levina, A.; Barr-David, G.; Codd, R.; Lay, P. A.; Dixon, N. E.; Hammershøi, A.; Hendry, P. *Chem. Res. Toxicol.* **1999**, *12*, 371−381. Lay, P. A.; Levina, A.; Dixon, N. E. *Inorg. Chem.*, submitted for publication.
(33) Dillon, C. T.; Lay, P. A.; Bonin, A. M.; Cholewa, M.; Legge, G. J. F.; Collins, T. J.; Kostka, K. L. *Chem. Res. Toxicol.* **1998**, *11*, 119−129.
(34) Branca, M.; Micera, G.; Segre, U.; Dessí, A. *Inorg. Chem.* **1992**, *31*, 2404−2408.
(35) Derouane, E. G.; Ouhadi, T. *Chem. Phys. Lett.* **1975**, *31*, 70−74.
(36) Bramley, R.; Ji, J.-Y.; Lay, P. A. *Inorg. Chem.* **1991**, *30*, 1557−1564.
(37) Irwin, J. A., Ph.D. Thesis, The University of Sydney, 1998.
(38) Quiros, M.; Goodgame, D. M. L. *Polyhedron* **1992**, *11*, 1−5.
(39) Signorella, S.; Rizzotto, M.; Daier, V.; Frascaroli, M. I.; Palopoli, C.; Martino, D.; Bousseksou, A.; Sala, L. F. *J. Chem. Soc., Dalton Trans.* **1996**, 1607−1611.
(40) Liu, K. J.; Shi, X.; Jiang, J.; Goda, F.; Dalal, N.; Swartz, H. M. *Ann. Clin. Lab. Sci.* **1996**, *26*, 176−184.
(41) Barr-David, G.; Charara, M.; Codd, R.; Farrell, R. P.; Irwin, J. A.; Lay, P. A.; Bramley, R.; Brumby, S.; Ji, J.-Y.; Hanson, G. R. *J. Chem. Soc., Faraday Trans.* **1995**, *91*, 1207−1216.
(42) Rao, C. P.; Kaiwar, S. P. *Carbohydr. Res.* **1993**, *244*, 15−25.
(43) Kaiwar, S. P.; Raghavan, M. S. S.; Rao, C. P. *Carbohydr. Res.* **1994**, *256*, 29−40.
(44) Branca, M.; Dessí, A.; Kozlowski, H.; Micera, G.; Swiatek, J. *J. Inorg. Biochem.* **1990**, *39*, 217−226.
(45) Signorella, S. R.; Santoro, M. I.; Mulero, M. N.; Sala, L. F. *Can. J. Chem.* **1994**, *72*, 398−402.
(46) Branca, M.; Micera, G.; Dessí, A. *Inorg. Chim. Acta* **1988**, *153*, 61−65.
(47) Sala, L. F.; Signorella, S. R.; Rizzotto, M.; Frascaroli, M. I.; Gandolfo, F. *Can. J. Chem.* **1992**, *70*, 2046−2052.
(48) Heiple, J. M.; Taylor, D. L. In *Intracellular pH: Its Measurement, Regulation and Utilization in Cellular Functions*; Nuccitelli, R., Deamer, D. W., Eds.; Alan R. Liss, Inc.: New York, 1982; pp 21−54.

are diol groups (e.g., ascorbic acid, ribose, D-glucose, and derivatives) and 2-hydroxy acids (e.g., citric, malic, and lactic acids). These different functional groups can be mimicked by different regions of qaH_5, which has a *tert*-2-hydroxy acid moiety in addition to a *cis*-diol (O^3,O^4) and a *trans*-diol (O^4,O^5) group. All of these functional groups are potential chelates for Cr(V). Therefore, this ligand enables intramolecular competition experiments to be conducted with regard to different functional groups (*tert*-2-hydroxy acid versus *vic*-diol) and different orientations within the same functional group (*cis*- versus *trans*-diol). A thorough understanding of the signature EPR spectra of the individual complexes formed between Cr(V) and these model ligands is important in terms of providing a basis for the interpretation of likely Cr(V) complexes formed in vivo and has important implications with respect to the better understanding of Cr(VI)-induced carcinogenesis.

Experimental Section

Chemicals. Quinic acid (qaH_5, ICN Biomedicals), shikimic acid (saH_4, Sigma, 99%), glutathione (GSH, Aldrich, 96%), $hmbaH_2$ (Aldrich, 98%), $ehbaH_2$ (Aldrich, 98%), $K_2Cr_2O_7$ (Merck, GR), $Na_2Cr_2O_7 \cdot 2H_2O$ (Merck, GR), $Na(CH_3)_2AsO_2 \cdot H_2O$ (Aldrich, 98%), methanol (Ajax, AR Grade), acetone (BDH, AR grade), and dimethyl sulfoxide (DMSO, Sigma, 99.5%) were used as received. All aqueous solutions were prepared using distilled water.

Syntheses. ***Caution:*** *$Na_2Cr_2O_7$ is carcinogenic,[2] and Cr(V)-2-hydroxy acid complexes are mutagenic[4] and potential carcinogens. These substances should be handled with due care, avoiding skin contact and inhalation of dust.*

(A) $K[Cr(O)(qaH_3)_2]\cdot H_2O$. Finely ground anhydrous $K_2Cr_2O_7$ (0.411 g, 1.40 mmol) was added to a solution of qaH_5 (1.609 g, 8.37 mmol) in methanol (500 mL), and the mixture was stirred for 2 h. The red−brown solution was filtered through a sintered-glass filter to remove unreacted $K_2Cr_2O_7$, and the volume of the filtrate was reduced to 85 mL via rotary evaporation (external bath <35 °C) at which point a finely divided red−brown powder appeared. The reaction solution was left at −22 °C overnight. The red−brown product was filtered, and the solid was washed with diethyl ether (2 × 25 mL) under a nitrogen atmosphere. Yield: 0.241 g (18.3%). Anal. calcd for $C_{14}H_{22}O_{14}CrK$: C, 33.27%; H, 4.39%; Cr, 10.29%; K, 7.74%. Found: C, 33.11%; H, 4.10%; Cr, 10.60%; K, 7.31%. FTIR (KBr matrix): 3300 (s, br), 2950 (w), 1684 (s), 1677 (s), 1444 (w), 1419 (w), 1336 (w), 1288 (m), 1263 (m), 1241 (m), 1157 (w), 1118 (m), 1070 (m), 1050 (m), 993 (s), 962 (w), 846 (w), 816 (m), 824 (m), 752 (w), 696 (m), 638 (m), 574 (w), 532 (w) cm^{-1}. UV/Vis (DMSO): λ, nm (ϵ, M^{-1} cm^{-1}) 436 sh (662), 554 (248). $\mu_{eff} = 2.10\ \mu_B$. CD (DMSO): λ, nm ($\Delta\epsilon$, deg M^{-1} m^{-1}) 338 (−0.8), 373 (−1.2), 437 (+9.8), 553 (−26.9).

(B) $Na[Cr(O)(hmba)_2]\cdot H_2O$ and $Na[Cr(O)(ehba)_2]\cdot H_2O$ were synthesized in acetone according to the literature method[29] and were microanalytically pure. The aqueous electronic absorption spectra of the complexes were also in agreement with previously reported data.[28,29]

Physical Measurements. Electronic absorption spectra were obtained on a Hewlett-Packard 8452A UV/vis diode array spectrometer. Fourier transform infrared spectra were recorded (DRIFTS protocol) on a Biorad FTS-40 FTIR spectrometer. Circular dichroism spectra were collected on a Jasco J-710C spectrometer, calibrated with NH_4-(+)-10-camphorsulfonate (JASCO Standard, 0.06% w/v in water). Analysis for K was undertaken by flame photometry (Corning 400 Flame meter) using KCl as the calibration standard. Magnetic susceptibility measurements were obtained using a Sherwood Scientific Magnetic Susceptibility Balance, which had been calibrated with $(NH_4)_2Fe(SO_4)_2 \cdot 6H_2O$ (Merck).

EPR Spectroscopic Measurements. Solution X-band EPR spectra (~9.6 GHz) at room temperature were recorded as the first derivative of absorption in quartz flat cells (Wilmad) using a Bruker ESP300 spectrometer linked to a Hewlett-Packard 5352B microwave frequency counter and a Bruker ERO35M NMR gaussmeter. Typically, spectra were a total of 5−10 scans and were acquired using the following conditions: modulation frequency = 100 kHz, modulation amplitude = 0.34 G, time constant = 1.28 ms, conversion time = 5.12 ms, and microwave power = 0.2 and 20 mW for the central Cr signal (sweep width = 15 G) and ^{53}Cr-hyperfine satellites (sweep width = 75 G), respectively. Second-order corrections were applied to obtain ^{53}Cr A_{iso} values. The spectra were converted into DOS format using Bruker software, and the files were imported into WINEPR[49] and WinSIM[50] for graphics and simulation purposes, respectively. A Bruker EMX 081 EPR spectrometer (X-band) linked to an EMX 032T field controller, and a Bruker EMX 035M gaussmeter was used for acquiring spectra of solid samples. The samples (~30 mg) were packed in quartz cylindrical tubes (Wilmad, i.d. = 1 mm, o.d. = 3 mm), and spectra (total of 5 scans, sweep width = 300 G, remaining conditions as described above) were collected at a power of 2 mW.

EPR Simulation. EPR spectra were simulated using the program PEST WinSIM.[50] The simulation procedure requires the input of the "*g* shift" (from center field, equivalent to g_{iso} value), line width, ^{1}H-superhyperfine coupling constants (^{1}H a_{iso}), and the number of equivalent protons (H_{eq}) for each hyperfine coupling constant. The simplex algorithm was used for spectral optimizations, and the line shape was set to 100% Lorentian in all cases. A simulation was deemed successful when the parameters for each unique Cr(V) species were found to be consistent within all simulations, with maximum deviations in the g_{iso} and ^{1}H a_{iso} values being ± 0.0001 units and $\pm 0.02 \times 10^{-4}$ cm^{-1}, respectively. Values for ^{1}H a_{iso} were included only where the ^{1}H a_{iso} value is greater than the LW (line width) of the species, since the signal was not significantly affected where the ^{1}H a_{iso} value was ≤0.5 LW. Simulations were not undertaken of the ^{53}Cr-hyperfine satellites.

General Procedure for EPR Measurements. Spectra were obtained from aqueous solutions of $K[Cr(O)(qaH_3)_2]\cdot H_2O$, or from reaction solutions of Cr(V)-qa or -sa species generated by the reduction of Cr(VI) by GSH in the presence of excess qaH_5 or saH_4, respectively. Spectra were acquired at t ~4 min after mixing the solutions. Aqueous stock solutions (0.1, 0.2 M) of GSH were prepared at the start of each series of experiments and were kept on ice between use. For experiments requiring conditions of a constant pH value, the qaH_5 stock solution either was self-buffering (qaH_5-qaH_4, pH ~4.0) or was prepared in cacodylate buffer (pH 6.4), using NaOH for pH adjustment in both instances. The pH values of bulk solutions (10 mL) were measured using an Activon pH meter (Model 210) with an Activon calomel pH probe (AEP 321). For small volumes (≤1 mL), the pH values were measured using a HANNA microcomputer pH meter (HI 9023) with a micro pH probe (HI 1083B).

EPR Spectra of $K[Cr(O)(qaH_3)_2]\cdot H_2O$. Spectra were obtained from aqueous solutions (1 mM) of $K[Cr(O)(qaH_3)_2]\cdot H_2O$ (pH 4.0) in the presence of excess qaH_5 ($[qaH_5]/[Cr(V)] = 2, 5, 20$). Two series (pH = 4.0 or 6.4) of EPR spectra were acquired from aqueous solutions of $K[Cr(O)(qaH_3)_2]\cdot H_2O$ in the presence of qaH_5, where the pH value and the $[qaH_5]/[Cr(V)]$ were kept constant {$[qaH_5]/[Cr(V)] = 2$ (2:1, 4:2, 10:5, 20:10)}. The temperature dependence of the aqueous EPR spectra of $K[Cr(O)(qaH_3)_2]\cdot H_2O$ (2 mM) was examined at 12, 17, 23, 31, 40, or 46 °C.

EPR Spectra of the Cr(VI)/GSH Reaction in the Presence of Excess qaH_5 or saH_4. Spectra were obtained from solutions of Cr(VI), GSH, and qaH_5 or saH_4, where the final concentrations of reactants were 40, 2, and 100 mM, respectively. The pH values of the solutions were adjusted using stock NaOH solutions, prior to making the final reaction solution to volume. Although the system was unbuffered, the variation in the pH values was negligible during the aging of the solution or spectral acquisition. Spectra were obtained at the following pH values: 2.71, 4.40, 5.45, 6.84, 7.52, 8.35, or 9.92 (saH_4) and 2.45, 4.17, 5.08, 6.18, 7.28, 8.17, or 9.40 (qaH_5). EPR spectra were also obtained from aqueous solutions of Cr(VI), GSH, and saH_4 (pH ~3.0), where the final concentrations of reactants were 40, 2, and either 100, 250, 500, or 800 mM, respectively. Additional series of EPR spectra were acquired from solutions of Cr(VI), GSH and saH_4 or qaH_5 where the $[saH_4]/[Cr(V)]$ or $[qaH_5]/[Cr(V)]$ was varied: $[saH_4]/[Cr(V)]$ 2.5, 6.25, 12.5, 20 (pH 6.8) or $[qaH_5]/[Cr(V)]$ 2.5, 10, 40, 80 (pH 6.9).

(49) WINEPR; Version 921201; Bruker-Franzen Analytic GmbH: Bremen, 1996.

(50) WinSIM *EPR Calculations for MS−Windows*; Version 0.96: National Institute of Environmental Health Sciences, 1995.

Results

K[Cr(O)(qaH$_3$)$_2$]·H$_2$O. The complex was isolated as a finely divided red−brown powder with a magnetic moment (μ_{eff} = 2.10 μ_B) indicating the presence of a single unpaired electron as for the Cr(V) ion (d^1). Consistent with Na[Cr(O)(hmba)$_2$] and Na[Cr(O)(ehba)$_2$] (μ_{eff} = 2.05 μ_B),[51] the magnetic moment of K[Cr(O)(qaH$_3$)$_2$]·H$_2$O, is slightly higher than the spin-only value. The FTIR spectrum of K[Cr(O)(qaH$_3$)$_2$]·H$_2$O shows a strong, sharp peak at 993 cm^{-1}, characteristic of $\nu_{Cr=O}$ of Cr(V)-2-hydroxy acid complexes.[51] The electronic absorption spectrum of K[Cr(O)(qaH$_3$)$_2$]·H$_2$O in DMSO is similar to that of Na[Cr(O)(hmba)$_2$]·H$_2$O (λ_{max} ∼550 nm) and also shows the definitive signature for Cr(V)-2-hydroxy acid complexes at λ ∼800 nm (ϵ ∼20 M^{-1} cm^{-1}).[51] Despite many attempts, crystals of K[Cr(O)(qaH$_3$)$_2$]·H$_2$O suitable for X-ray structural analysis have not been obtained as yet. It is possible that the complex may exist in the solid state as more than one geometric isomer as has been observed for similar complexes in solution.[52,53] The XAFS structure of [Cr(O)(qaH$_3$)$_2$]$^-$ is also consistent with a bis(2-hydroxy acid) coordination mode.[30,54] The solid-state EPR spectra of the Cr(V)-2-hydroxy acid complexes, K[Cr(O)(qaH$_3$)$_2$]·H$_2$O, Na[Cr(O)(hmba)$_2$]·H$_2$O and Na[Cr(O)(ehba)$_2$]·H$_2$O, exhibit a single broad signal (Figure 1, upper graphic) with comparable g_{iso} values (Table 1). The signal line widths vary among the spectra, in the following order of highest to lowest: K[Cr(O)(qaH$_3$)$_2$]·H$_2$O > Na[Cr(O)(hmba)$_2$]·H$_2$O > Na[Cr(O)(ehba)$_2$]·H$_2$O.

Solution EPR Spectra of [Cr(O)(L)$_2$]$^-$ (L = qaH$_3$, hmba, ehba) in Water. The central Cr signal of the EPR spectrum of an aqueous solution of K[Cr(O)(qaH$_3$)$_2$]·H$_2$O shows two symmetrical signals with g_{iso} = 1.9787 and g_{iso} = 1.9791 (Figure 1, middle graphic). The EPR spectra of the structurally analogous complexes, Na[Cr(O)(hmba)$_2$]·H$_2$O and Na[Cr(O)(ehba)$_2$]·H$_2$O, show singlets (g_{iso} = 1.9785 and g_{iso} = 1.9784, respectively), which are unsymmetric in the second-derivative plots. The presence of more than one species in the aqueous EPR spectra of all the complexes is unambiguously established from the ^{53}Cr-hyperfine satellite region, where two resolvable sets of signals are observed (Figure 1, lower graphic). The A_{iso} values of the two resolved species are very similar among K[Cr(O)(qaH$_3$)$_2$]·H$_2$O, Na[Cr(O)(hmba)$_2$]·H$_2$O, and Na[Cr(O)(ehba)$_2$]·H$_2$O (Table 1). The possibility of the multiple species in the case of Na[Cr(O)(hmba)$_2$]·H$_2$O (hmba has a chiral carbon) arising from chiral species, Na[Cr(O)(*R*-hmba)$_2$]·H$_2$O or Na[Cr(O)(*S*-hmba)$_2$]·H$_2$O, is discounted, since very similar spectra are obtained from solutions of Na[Cr(O)(hmba)$_2$]·H$_2$O and the achiral complex, Na[Cr(O)(ehba)$_2$]·H$_2$O. The two signals observed in the aqueous solution EPR spectra of Na[Cr(O)(L)$_2$]·H$_2$O (L = hmba, ehba) have been assigned as being due to geometric isomers,[52,53] and it is expected that geometric isomers are similarly observed for K[Cr(O)(qaH$_3$)$_2$]·H$_2$O.

[qaH$_5$]/[Cr(V)] Dependence on K[Cr(O)(qaH$_3$)$_2$]·H$_2$O Speciation at pH 4.0. The possibility of the two signals in the aqueous EPR spectra of K[Cr(O)(qaH$_3$)$_2$]·H$_2$O being due to mono-chelate and bis-chelate Cr(V)-qa species was addressed by examining the effect of [qaH$_5$] at constant pH (4.0 ± 0.1, Figure S1, Supporting Information). The independence of the spectra on [qaH$_5$] shows that all of the species present are bis chelate complexes.

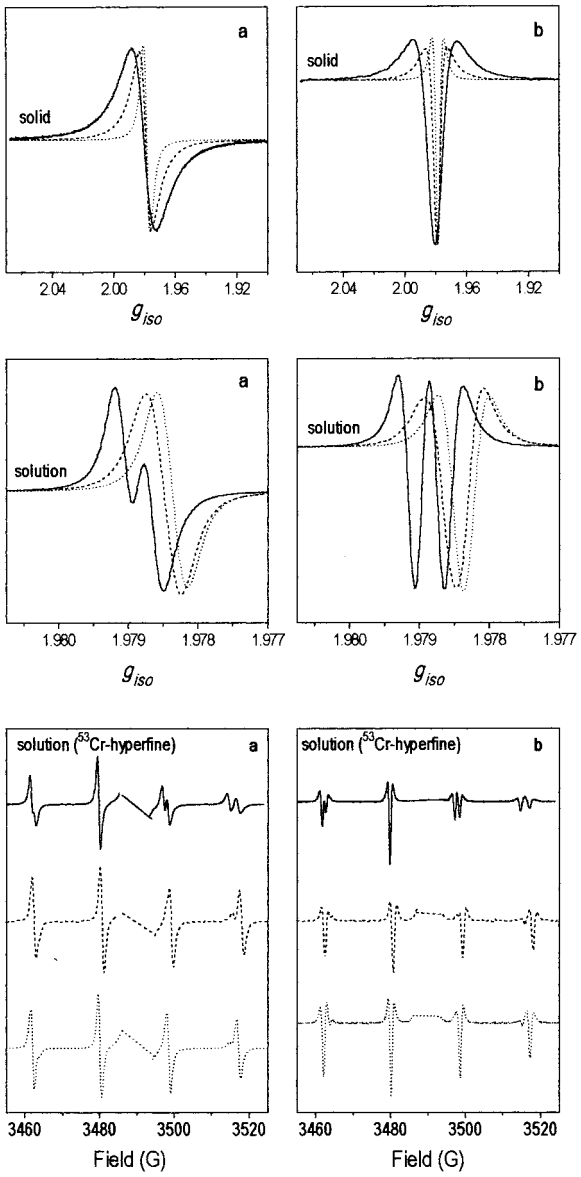

Figure 1. Room temperature X-band EPR spectra (∼20 °C) of K[Cr(O)(qaH$_3$)$_2$]·H$_2$O (solid line), Na[Cr(O)(hmba)$_2$]·H$_2$O (dashed line), and Na[Cr(O)(ehba)$_2$]·H$_2$O (dotted line) in the solid state (upper graphic, central Cr signal) and in aqueous solution (middle graphic, central Cr signal; lower graphic, ^{53}Cr-hyperfine signals), presented as (a) first- and (b) second-derivative plots.

[Cr(V)] Dependence on K[Cr(O)(qaH$_3$)$_2$]·H$_2$O Speciation at Constant [qaH$_5$]/[Cr(V)] and pH 4.0 or 6.4. A small increase in the height of the signal at g_{iso} = 1.9787 compared to that at g_{iso} = 1.9791 was apparent as the total concentration is increased (Figure S2); however, this was due to the concentration-dependent line broadening. Two independent simulation procedures {(1) the concentration of each species was frozen (50%) and the line width was allowed to vary; (2) the concentrations of the species were varied, while the line widths (0.43 G) were kept constant) showed that the relative intensities of the two signals were independent of increasing [qaH$_5$]/[Cr(V)], where both the [qaH$_5$]/[Cr(V)] and the pH value were constants. A similar invariance in the ratio of the EPR signals (Figure S3) was obtained at pH 6.4. Therefore, the possibility that different EPR signals for K[Cr(O)(qaH$_3$)$_2$]·H$_2$O

(51) Farrell, R. P.; Lay, P. A. *Comments Inorg. Chem.* **1992**, *13*, 133−175.
(52) Bramley, R.; Ji, J.-Y.; Judd, R. J.; Lay, P. A. *Inorg. Chem.* **1990**, *29*, 3089−3094.
(53) Branca, M.; Dessí, A.; Micera, G.; Sanna, D. *Inorg. Chem.* **1993**, *32*, 578−581.
(54) Codd, R.; Levina, A.; Zhang, L.; Hambley, T. W.; Lay, P. A. *Inorg. Chem.*, submitted for publication.

Table 1. EPR Spectroscopic Parameters, g_{iso}, A_{iso}, and Line Widths (LW), for $K[Cr(O)(qaH_3)_2]\cdot H_2O$, $Na[Cr(O)(ehba)_2]\cdot H_2O$, and $Na[Cr(O)(hmba)_2]\cdot H_2O$ in Aqueous Solution and in the Solid State

	solution						solid	
	species I			species II				
complex	g_{iso}	LW[a] (G)	A_{iso}[b]	g_{iso}	LW[a] (G)	A_{iso}[b]	g_{iso}	LW[a] (G)
$[Cr(O)(ehba)_2]^-$	1.9784	0.78	17.2	1.9784[c]	0.78[c]	16.1	1.9783	7.8
$[Cr(O)(hmba)_2]^-$	1.9785	0.91	17.4	1.9784[c]	0.91[c]	16.3	1.9790	14.6
$[Cr(O)(qaH_3)_2]^-$	1.9787	0.49	17.2	1.9791	0.45	16.4	1.9803	30.4

[a] LW = line width. [b] A_{iso} units = 10^{-4} cm^{-1}. [c] The g_{iso} values and the line widths of the individual species are unable to be distinguished.

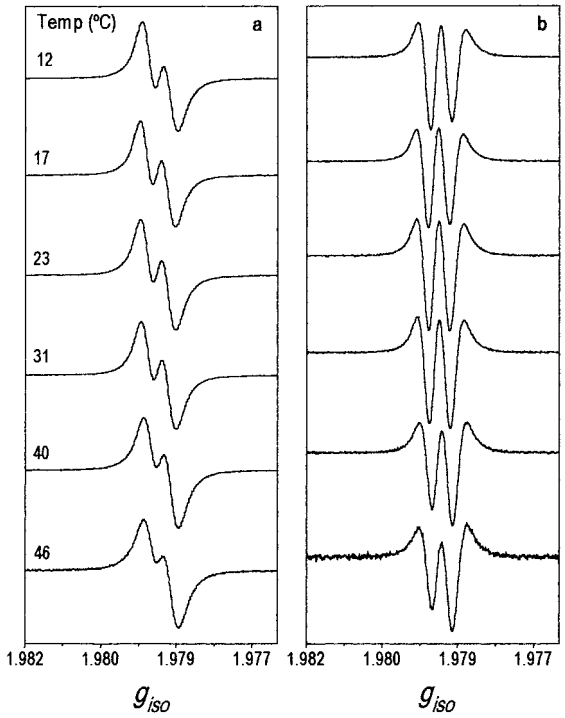

Figure 2. X-band EPR spectra of $K[Cr(O)(qaH_3)_2]\cdot H_2O$ in water as a function of temperature (°C), presented as (a) first- and (b) second-derivative plots.

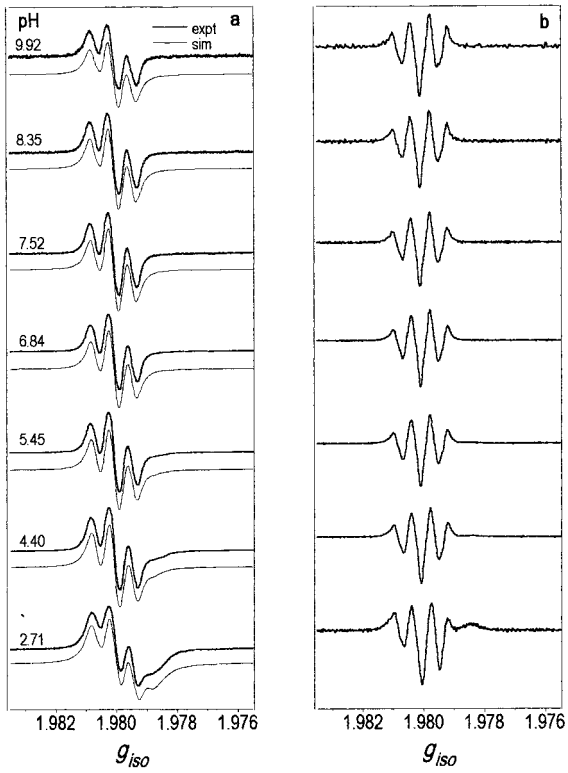

Figure 3. Room temperature X-band EPR spectra (~20 °C) of the Cr(V) intermediates in the reaction of Cr(VI) (40 mM) with GSH (2 mM) in the presence of saH_4 (100 mM) in water at pH 2.71, 4.40, 5.45, 6.84, 7.52, 8.35, or 9.92, presented as (a) first- (expt and sim) and (b) second-derivative plots.

were due to mononuclear $[Cr(O)(qaH_3)_2]^-$ and polymeric $[Cr(O)(\mu\text{-qaH})]_n^{m-}$ complexes was eliminated.

Temperature Dependence of $K[Cr(O)(qaH_3)_2]\cdot H_2O$ Speciation in Water. The intensity of the signal at $g_{iso} = 1.9787$ increased relative to that at $g_{iso} = 1.9791$, with increasing temperature (Figure 2). The linear plot of $\ln\{[g_{iso}(1.9787)]/[g_{iso}(1.9791)]\}$ versus $1/T$ (Figure S4) gave $\Delta H°$ and $\Delta S°$ values of 5.4 kJ mol^{-1} and 11.0 J K^{-1} mol^{-1}, respectively. The small values of $\Delta H°$ and $\Delta S°$ suggest that the coordination groups of the two species are similar.

pH Dependence of Cr(V)-sa Speciation. The EPR spectra obtained upon the reduction of Cr(VI) by GSH in the presence of excess saH_4 exhibited (where the pH value > 5.5) a triplet with $g_{iso} = 1.9801$ and ^1H $a_{iso} = 0.95 \times 10^{-4}$ cm^{-1} (Figure 3). There is very little change in the spectra upon increasing the pH values from 6.84 to 9.92. The ^{53}Cr-hyperfine satellites are well resolved (Figure S5) with $A_{iso} = 16.6 \times 10^{-4}$ cm^{-1}. The g_{iso} and A_{iso} values agree closely to the expected values ($g_{iso} = 1.9800$, $A_{iso} = 16.5 \times 10^{-4}$ cm^{-1}) for a five-coordinate oxo-Cr(V) species with four alcoholato donors.[41] At pH values < 4.5, an additional broad signal is observed at g_{iso} ~1.9792. As the pH increases, the relative concentration of this signal decreases, compared to the signals at higher g_{iso} values. The second-derivative plots of the spectra of both the central Cr signal (Figure 3) and the ^{53}Cr-hyperfine region (Figure S5) show that the triplet signal (at pH values > 5.5) is slightly unsymmetric, which suggests the presence of more than one species. It is possible, for example, that the species giving rise to the triplet exists as more than one geometric isomer. The ^1H a_{iso} value (0.95×10^{-4} cm^{-1}) suggests that the dominant Cr(V)-sa species involves coordination to the *cis*-diol (3,4-) group of the ligand, by analogy with EPR spectral simulation of Cr(V)-*cis*-1,2-cyclohexanediol complexes (^1H $a_{iso} = \sim 0.9 \times 10^{-4}$ cm^{-1}).[37] Since saH_4 has two pairs of *vic*-diol groups (3,4- and 4,5-), the possibility of the presence of other linkage isomers cannot be discounted, although a somewhat more complicated EPR spectrum would be expected if alternative linkage isomers were present in significant concentrations.

[saH_4]/[Cr(VI)] Dependence on Cr(V) Speciation at Constant pH Values. The possibility of an equilibrium existing between mono- and bis-chelate Cr(V)-sa species was eliminated by the lack of change in the spectrum with increasing [saH_4]/[Cr(V)], at pH 6.8 (Figure S6). The slight asymmetry of the central Cr signal is well simulated assuming the presence of two triplets, (g_{iso} (i) = 1.9800, ^1H $a_{iso} = 0.94 \times 10^{-4}$ cm^{-1}, rel. concn = 45.05%; g_{iso} (ii) = 1.9801, ^1H $a_{iso} = 0.97 \times 10^{-4}$ cm^{-1}, rel. concn = 54.95%) in which the g_{iso} values differ by 0.0001 units. At pH values < 5.5 a broad shoulder appears in

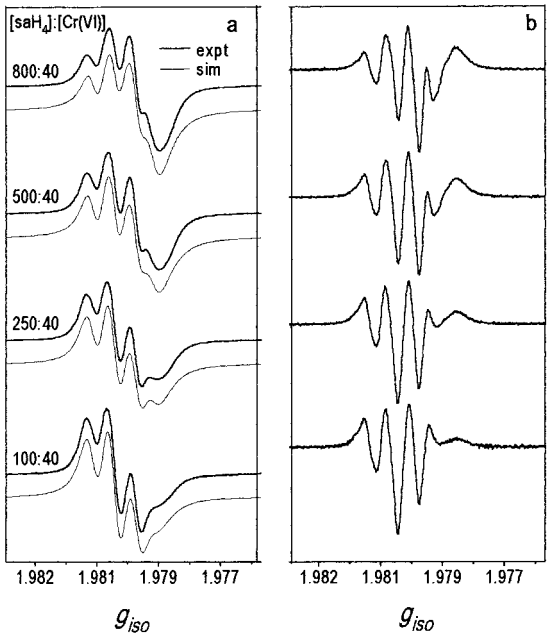

Figure 4. Room temperature (~20 °C) X-band EPR spectra of the Cr(V) intermediates in the reaction of Cr(VI) (40 mM) with GSH (2 mM) in the presence of saH_4 (100, 250, 500, or 800 mM), presented as (a) first- (expt and sim) and (b) second-derivative plots; ratio of $[saH_4]/[Cr(VI)]$ (pH) = 2.5 (2.94), 6.25 (2.97), 12.5 (2.97), or 20 (3.01).

the Cr(V)-sa spectra, centered at $g_{iso} = 1.9792$ (Figure 3), which was further investigated by varying $[saH_4]/[Cr(VI)]$ at constant pH (Figure 4). In this case, the intensity of the signal at the lower g_{iso} value increases, relative to that of the signals at $g_{iso} = 1.9800$ and $g_{iso} = 1.9801$. Since the relative concentration of the signal at $g_{iso} = 1.9792$ increases with increasing $[saH_4]$ compared to the bis-chelate Cr(V)-sa species, the former signal must be due to species which have a ligand-to-metal ratio >2.

Equilibrium Constants for Speciation of Cr(V)-sa Complexes. The spectra were simulated as two triplets, representing the purported geometric isomers of $[Cr(O)(O^3,O^4\text{-}saH)_2]^{3-}$ and one doublet ($g_{iso} = 1.9792$, ^1H $a_{iso} = 0.82 \times 10^{-4}$ cm^{-1}). The pH and $[saH_4]$ dependence of the Cr(V)-sa system fit the equilibrium shown in eq 1, where A = bis-chelate Cr(V)-sa species (trianionic) and B = tris-sa Cr(V) species (dianionic). The ligand concentration dependence study was conducted at pH values < pK_a of saH_4 (4.01),[55] and therefore, only a first-order dependence on $[H^+]$ is expected.

$$A + saH_4 + H^+ \overset{K_1}{\rightleftharpoons} B; \quad K_1 = \frac{[B]}{[A][saH_4][H^+]} \qquad (1)$$

A plot of $[B]/([A][H^+])$ versus $[saH_4]$ is linear with a slope of K_1 and an intercept close to the origin (Figure S7). The values of K_1 for the formation of the putative tris-sa Cr(V) species ($g_{iso} = 1.9792$) are on the order of 6×10^3 M^{-2} (Table S1). Values for K_1 calculated at pH 2.71 from eq 1 were of a magnitude similar to that obtained above. It is possible that the putative tris-sa Cr(V) species exists as more than one geometric isomer, although for the simulation, the species was treated as a single isomer.

pH Dependence of Cr(V)-qa Speciation. At low pH values (2.45, 4.17), the EPR spectra of the Cr(VI)/GSH reaction in the presence of qaH_5 (Figure 5, central signal, and Figure S8, ^{53}Cr-hyperfine satellites) are the same as those observed from an aqueous solution of $K[Cr(O)(qaH_3)_2]\cdot H_2O$. As the pH value increases, additional signals are observed at g_{iso} values ~1.9794. At pH 9.40, a broad triplet appears at $g_{iso} = 1.9801$, similar to that observed for the Cr(V)-sa species. Concomitant with the appearance of new signals with increasing pH values, the relative intensity of the signal at $g_{iso} = 1.9787$ decreases. The signals appearing at intermediate pH values (between pH 5.1 and 7.3) may be due to bis-chelate Cr(V)-qa species with donation occurring via one 2-hydroxy acid group and one diol group. A donor set of this type would be expected to yield a Cr(V) species with a higher g_{iso} value, compared to a bis(2-hydroxy acid) Cr(V) species.[41] Additional minor signals appeared when the pH value was > 6 (Figure 5). These signals ($g_{iso} = 1.9751$, 1.9762, 1.9768, and 1.9776) are just perceptible at pH 6.18 and increase in intensity at pH 6.91. The minor signals are more clearly observed in the second-derivative plot of the ^{53}Cr-hyperfine region of the EPR spectrum at pH 6.18 (Figure S8).

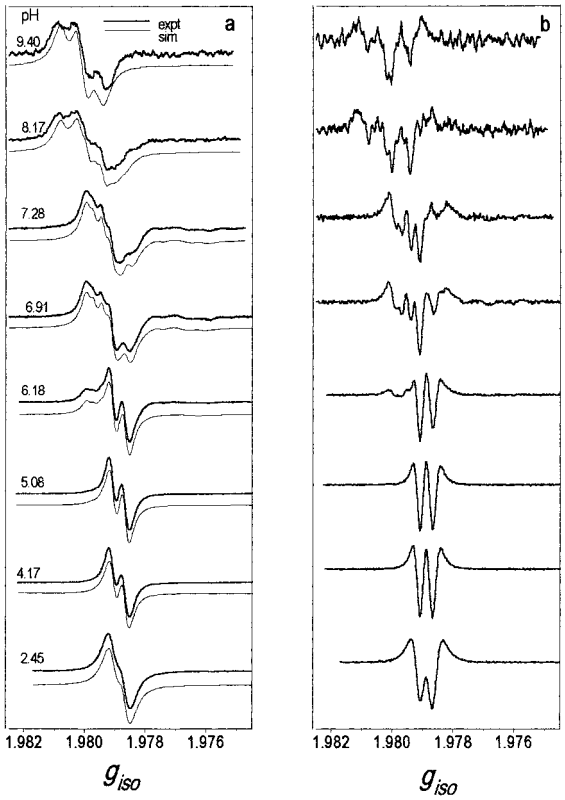

Figure 5. Room temperature (~20 °C) X-band EPR spectra of the Cr(V) intermediates in the reaction of Cr(VI) (40 mM) with GSH (2 mM) in the presence of qaH_5 (100 mM) at pH 2.45, 4.17, 5.08, 6.18, 6.91, 7.12, 8.17, or 9.40; presented as (a) first- (expt and sim) and (b) second-derivative plots.

Ligand Exchange and Geometric Isomerization Equilibrium Constants in the Cr(V)-qaH_m System. The spectra obtained at pH values between 2.45 and 7.28 were simulated as the linkage isomers $[Cr(O)(O^1,O^7\text{-}qaH_3)_2]^-$, $[Cr(O)(O^1,O^7\text{-}qaH_3)(O^3,O^4\text{-}qaH_2)]^{2-}$, and $[Cr(O)(O^1,O^7\text{-}qaH_2)(O^4,O^5\text{-}qaH_2)]^{2-}$ and two geometric isomers of each linkage isomer. At pH 8.17, these species were assumed to be present together with the bis-diol linkage isomer, $[Cr(O)(O^3,O^4\text{-}qaH_2)_2]^{3-}$ (as two geometric isomers). At pH 9.40 the spectrum was simulated as two triplets, representing the two geometric isomers of $[Cr(O)(O^3,O^4\text{-}qaH_2)_2]^{3-}$. The inclusion of the alternative bis-diol linkage isomers, $[Cr(O)(O^3,O^4\text{-}qaH_2)(O^4,O^5\text{-}qaH_2)]^{3-}$ and $[Cr(O)(O^4,O^5\text{-}qaH_2)_2]^{3-}$, did not improve the fit to the experimental data. Therefore, the latter two linkage isomers may be present only in very small concentrations, which is consistent with the

(55) Lamy, I.; Seywert, M.; Cromer, M.; Scharff, J.-P. *Anal. Chim. Acta* **1985**, *176*, 201−212.

Table 2. Values of the Observed and Calculated[41] EPR Spectroscopic Parameters, g_{iso}, ^{1}H a_{iso}, and A_{iso}, for Cr(V)-qa Linkage Isomers (Two Geometric Isomers per Linkage Isomer) Generated from the Cr(VI)/GSH/qaH$_5$ Reaction

	g_{iso}		^{1}H a_{iso}[a]	A_{iso} (10^{-4} cm^{-1})	
species	expt	calc	[N^{o}of H$_{eq}$][b]	expt	calc
[Cr(O)(O^1,O^7-qaH$_3$)$_2$]$^-$	1.9787	1.9783		17.2	16.7
[Cr(O)(O^1,O^7-qaH$_3$)$_2$]$^-$	1.9791	1.9783		16.4	16.7
[Cr(O)(O^1,O^7-qaH$_3$)(O^3,O^4-qaH$_2$)]$^{2-}$	1.9791	1.9791	0.83 [1]	16.4[c]	16.6
[Cr(O)(O^1,O^7-qaH$_3$)(O^3,O^4-qaH$_2$)]$^{2-}$	1.9794	1.9791	0.85 [1]	16.4[c]	16.6
[Cr(O)(O^1,O^7-qaH$_3$)(O^4,O^5-qaH$_2$)]$^{2-}$	1.9794	1.9791		16.4[c]	16.6
[Cr(O)(O^1,O^7-qaH$_3$)(O^4,O^5-qaH$_2$)]$^{2-}$	1.9799	1.9791		16.4[c]	16.6
[Cr(O)(O^3,O^4-qaH$_2$)$_2$]$^{3-}$	1.9800	1.9800	0.84 [2]	ND[d]	16.5
[Cr(O)(O^3,O^4-qaH$_2$)$_2$]$^{3-}$	1.9802	1.9800	0.85 [2]	ND[d]	16.5

[a] ^{1}H a_{iso} units = 10^{-4} cm^{-1}. [b] Number of magnetically equivalent protons. [c] The A_{iso} value for each individual mixed-linkage isomer is unable to be distinguished. [d] ND = not determined. The ^{53}Cr-hyperfine signals were too weak to allow accurate determination of A_{iso} values.

Table 3. Values of the Equilibrium Constants, K_2,[a] for the Formation of Cr(V)-qa Linkage Isomers (Two Geometric Isomers per Linkage Isomer) from the Cr(VI)/GSH/qaH$_5$ Reaction

A	g_{iso}	B	g_{iso}	K_2 (M)
[Cr(O)(O^1,O^7-qaH$_3$)$_2$]$^-$	1.9787[b]	[Cr(O)(O^1,O^7-qaH$_3$)(O^3,O^4-qaH$_2$)]$^{2-}$	1.9791	1.2×10^{-7}
[Cr(O)(O^1,O^7-qaH$_3$)$_2$]$^-$	1.9787[b]	[Cr(O)(O^1,O^7-qaH$_3$)(O^3,O^4-qaH)$_2$]$^{2-}$	1.9794	2.1×10^{-7}
[Cr(O)(O^1,O^7-qaH$_3$)$_2$]$^-$	1.9787[b]	[Cr(O)(O^1,O^7-qaH$_3$)(O^4,O^5-qaH$_2$)]$^{2-}$	1.9794	4.6×10^{-8}
[Cr(O)(O^1,O^7-qaH$_3$)$_2$]$^-$	1.9787[b]	[Cr(O)(O^1,O^7-qaH$_3$)(O^4,O^5-qaH$_2$)]$^{2-}$	1.9799	4.0×10^{-8}

[a] From eq 2, $K_2 = ([D][H^+])/[C]$ and a plot of [D]/[C] vs $1/[H^+]$ will yield a straight line of slope K_2 and intercept = 0. [b] The relative concentrations of the purported geometric isomers of [Cr(O)(O^1,O^7-qaH$_3$)$_2$]$^-$ are equal. Therefore, for the calculation of equilibrium constants, the concentration of either isomer (g_{iso} = 1.9787 or 1.9791) can be used.

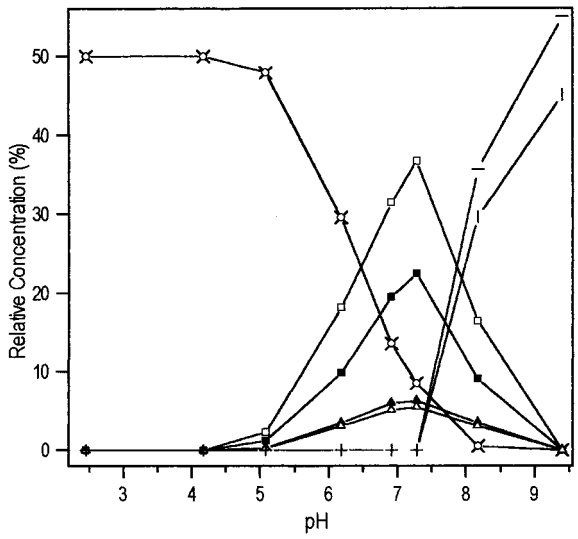

Figure 6. Relative concentrations of Cr(V)-qa linkage isomers as determined from EPR spectral simulation,[50] generated from reactions of Cr(VI) with GSH in the presence of qaH$_5$, as a function of pH. Two geometric isomers have been included per linkage isomer. Legend: × [Cr(O)(O^1,O^7-qaH$_3$)$_2$]$^-$ (g_{iso} = 1.9787); ○ [Cr(O)(O^1,O^7-qaH$_3$)$_2$]$^-$ (g_{iso} = 1.9791); ■ [Cr(O)(O^1,O^7-qaH$_3$)(O^3,O^4-qaH$_2$)]$^{2-}$ (g_{iso} = 1.9791); □ [Cr(O)(O^1,O^7-qaH$_3$)(O^3,O^4-qaH$_2$)]$^{2-}$ (g_{iso} = 1.9794); ▲ [Cr(O)(O^1,O^7-qaH$_3$)(O^4,O^5-qaH$_2$)]$^{2-}$ (g_{iso} = 1.9794); △ [Cr(O)(O^1,O^7-qaH$_3$)(O^4,O^5-qaH$_2$)]$^{2-}$ (g_{iso} = 1.9799); | [Cr(O)(O^3,O^4-qaH$_2$)$_2$]$^{3-}$ (g_{iso} = 1.9800); — [Cr(O)(O^3,O^4-qaH$_2$)$_2$]$^{3-}$ (g_{iso} = 1.9802).

predominance of the [Cr(O)(O^3,O^4-saH)$_2$]$^{3-}$ linkage isomer found in the Cr(V)-sa system. The EPR parameters of the species proposed for the Cr(V)-qa system are given in Table 2, and the relative concentrations of the species as a function of pH are shown in Figure 6. The equilibrium constants for the formation of the 2-hydroxy acid-diol Cr(V)-qa mixed-linkage isomers can be deduced from a plot of [D]/[C] versus $1/[H^+]$ according to eq 2, where C = [Cr(O)(O^1,O^7-qaH$_3$)$_2$]$^-$ and D = [Cr(O)(O^1,O^7-qaH$_3$)(O^3,O^4-qaH$_2$)]$^{2-}$ (two geometric isomers: D_1, D_2) or [Cr(O)(O^1,O^7-qaH$_3$)(O^4,O^5-qaH$_2$)]$^{2-}$ (two geometric isomers: D_3, D_4) (Figure S9).

$$C \overset{K_2}{\rightleftharpoons} D + H^+; \quad K_2 = \frac{[D][H^+]}{[C]} \tag{2}$$

$$D \overset{K_3}{\rightleftharpoons} E + H^+; \quad K_3 = \frac{[E][H^+]}{[D]} \tag{3}$$

The slope of the line represents K_2 and is on the order of 10^{-7} and 10^{-8} M for [Cr(O)(O^1,O^7-qaH$_3$)(O^3,O^4-qaH$_2$)]$^{2-}$ and [Cr(O)(O^1,O^7-qaH$_3$)(O^4,O^5-qaH$_2$)]$^{2-}$, respectively (Table 3). In both instances, the intercept is 0 within experimental error, as expected from such simple equilibria. The equilibrium constants, K_3, for the formation of isomers of [Cr(O)(O^3,O^4-qaH$_2$)$_2$]$^{3-}$ [E] (eq 3) are on the order of 10^{-8} M. These values, however, should be treated with caution, since the plot of [E]/[D] versus $1/[H^+]$ only has two data points.

[qaH$_5$]/[Cr(VI)] Dependence on Cr(V) Speciation at pH 6.9. The effect of the ligand-to-metal ratio on the speciation of Cr(V)-qa complexes was examined by varying [qaH$_5$]/[Cr(VI)] at pH 6.91. The relative signal intensity due to [Cr(O)(O^1,O^7-qaH$_3$)$_2$]$^-$ appears to increase relative to the other signals with increasing [qaH$_5$]/[Cr(VI)], which indicates the presence of an equilibrium between mono- and bis-chelate Cr(V)-qa species (Figure S10). The relative changes in the signal intensities as a function of ligand-to-metal ratio, however, are very small, as shown by EPR spectral simulation.

Discussion

Quinic acid features a *tert*-2-hydroxy acid group, and two pairs of *vic*-diol groups orientated in a *cis*-(3,4-) and *trans*-(4,5-) fashion. The energetically favored conformation of qaH$_5$ is the chair conformation (as shown), where the 1-OH group is in the axial position.[56] The conformation of shikimic acid is similar to that of qaH$_5$, with the difference being a single point of

(56) Corse, J.; Lundin, R. E.; Sondheimer, E.; Waiss, A. C., Jr. *Phytochemistry* **1966**, *5*, 767−776.

unsaturation [C(1)−C(2)] in the cyclohexane ring. Stabilization of Cr(V) by saH_4 is most likely to involve the 3,4- and 4,5-diol regions of the molecule, although chelation via the carboxylato group is also possible.

$K[Cr(O)(qaH_3)_2]\cdot H_2O$. The isolation of this complex and its aqueous chemistry has wide reaching implications for understanding competition between the coordination of cyclic-diol (e.g., carbohydrates) and 2-hydroxy acid groups to transition metal ions in vivo. It has been proposed, on the basis of EPR spectra of Cr(V)-sugar complexes that, due to the bulk of carbohydrates, only mono-chelate Cr(V)-carbohydrate complexes can be formed.[44,46,47] The isolation of $K[Cr(O)(qaH_3)_2]\cdot H_2O$ with the carbohydrate-like ligand, qaH_5, illustrates that this is not necessarily the case. Also, extensive EPR spectroscopic experiments of the species formed between Cr(V) and D-glucose have shown that bis-chelate Cr(V)-D-glucose complexes are readily formed in the presence of excess ligand.[37,41] In addition to the 2-hydroxy acid coordination mode exhibited by qaH_5 in $[Cr(O)(qaH_3)_2]^-$, the *vic*-diol groups of the ligand are also potential chelates, giving rise to six potential Cr(V)-qa linkage isomers (**III**−**VIII**). The mixed-valence trinuclear vanadium complex, $(NH_4)_2\{[V^V(O)_2]_2[V^{IV}(O)](\mu\text{-}qaH_2)_2\}\cdot H_2O$, for example, features **I** coordinated via both the 2-hydroxy acid moiety and the 3-OH group.[57]

$[Cr(O)(qaH_m)_2]^{n-}$ Speciation. The two EPR signals of $K[Cr(O)(qaH_3)_2]\cdot H_2O$ at $g_{iso} = 1.9787$ and $g_{iso} = 1.9791$ are due to different species of the bis-(2-hydroxy acid) linkage isomer. This is established by the pH, [Cr(V)] and [Cr(V)]/[qaH_5] dependencies, and the distinct A_{iso} values (A_{iso} (**IIIa**) $= 17.2 \times 10^{-4}$ cm^{-1}; A_{iso} (**IIIb**) $= 16.4 \times 10^{-4}$ cm^{-1}). The A_{iso} values are similar to those observed in the EPR spectra from aqueous solutions of $Na[Cr(O)(ehba)_2]\cdot H_2O$ ($A_{iso} = 17.2 \times 10^{-4}$ cm^{-1}; $A_{iso} = 16.1 \times 10^{-4}$ cm^{-1}) and $Na[Cr(O)(hmba)_2]\cdot H_2O$ ($A_{iso} = 17.4 \times 10^{-4}$ cm^{-1}; $A_{iso} = 16.3 \times 10^{-4}$ cm^{-1}), which have been assigned previously to the presence of more than one geometric isomer per Cr(V)-2-hydroxy acid complex.[52,53] The presence of a maximum of three geometric isomers for Cr(V)-2-hydroxy acid complexes arises from the interchange of the alcoholato and/or the carboxylato donors about the distorted trigonal bipyramid.[52] The possibility of an equilibrium existing between mononuclear and polymeric species, where coordination features qaH bridging two Cr(V) ions via the 2-hydroxy acid group (O^1,O^7) and either the 4,5- (O^4,O^5) (**IX**) or 3,4- (O^3,O^4) diol groups (**X**) were eliminated due to the EPR spectral invariance upon changing the concentrations of qaH_5 and Cr(V) at a constant [qaH_5]/[Cr(V)] ratio and a constant pH value.

Linkage Isomerism in $[Cr(O)(qaH_m)_2]^{n-}$. The six different linkage isomers of $[Cr(O)(qaH_m)_2]^{n-}$, involving 2-hydroxy acid (O^1,O^7) and/or diol (O^3,O^4; O^4,O^5) chelation (**III**−**VIII**), would give rise to EPR signals with distinct g_{iso} and ^1H a_{iso} values. The complexes featuring coordination to one 2-hydroxy acid and one diol group, or to two diol groups, are most likely to be dianionic and trianionic, respectively, since the uncoordinated carboxylic acid group would be deprotonated at the pH values studied. The Cr(V) and the isoelectronic V(IV) ions show a marked preference for binding to *cis*- rather than *trans*-diol groups of sugars and 1,2-cyclohexanediol.[37,58,59] Also, the EPR spectral multiplicity of bis-chelate complexes formed between Cr(V) and either cis- or *trans*-cyclic-diol ligands will exhibit a

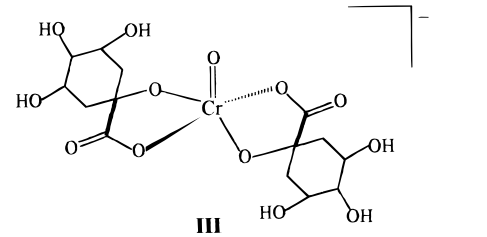

III

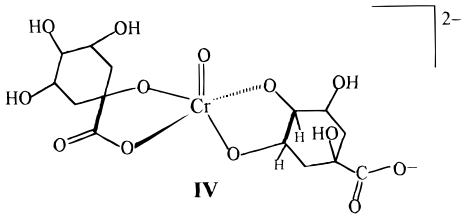

IV

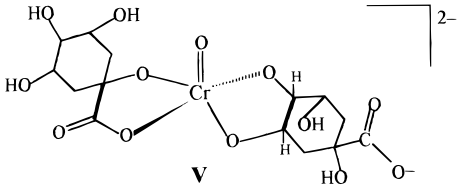

V

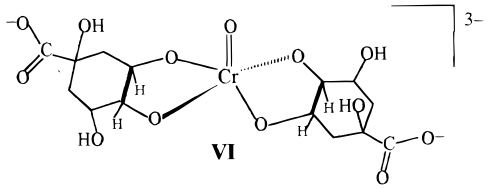

VI

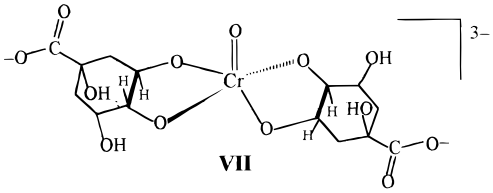

VII

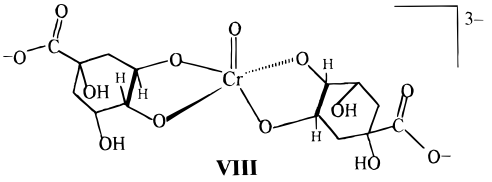

VIII

triplet and singlet, respectively, arising from the orientation of the ring protons of the coordinated diol groups with respect to the basal plane of the complex.[37] On the basis of this, the EPR spectra of $[Cr(O)(O^1,O^7\text{-}qaH_3)_2]^-$ (**III**), $[Cr(O)(O^1,O^7\text{-}qaH_3)(O^3,O^4\text{-}qaH_2)]^{2-}$ (**IV**), and $[Cr(O)(O^1,O^7\text{-}qaH_3)(O^4,O^5\text{-}qaH_2)]^{2-}$ (**V**) would exhibit a singlet, a doublet, and a singlet, respectively. Also, the concentration of **V** relative to **IV** would be expected to be small. As an alternative to the simulation of the EPR signals of $K[Cr(O)(qaH_3)_2]\cdot H_2O$ in water as two geometric isomers, a singlet ($g_{iso} = 1.9787$, rel. concn = 24.4%), a doublet ($g_{iso} = 1.9788$, ^1H $a_{iso} = 0.79 \times 10^{-4}$ cm^{-1}, rel. concn = 59.8%) and a singlet ($g_{iso} = 1.9790$, rel. concn = 15.8%) could be used. In such an analysis, the g_{iso} values for the putative **IV** and **V** isomers are higher than that for **III**, which is to be expected on the basis of an empirically derived set of EPR parameters for specific donors.[41] The trend in the g_{iso} values is also consistent with the higher g_{iso} value observed for $[Cr(O)(ehba)(ed)]^-$ (ed = 1,2-ethanediolato(2−)) compared to $[Cr(O)(ehba)_2]^-$.[36] How-

(57) Codd, R.; Hambley, T. W.; Lay, P. A. *Inorg. Chem.* **1995**, *34*, 877−882.

(58) Micera, G.; Dessí, A.; Sanna, D. *Inorg. Chem.* **1996**, *35*, 6349−6352.

(59) Branca, M.; Micera, G.; Dessí, A.; Sanna, D. *J. Inorg. Biochem.* **1992**, *45*, 169−177.

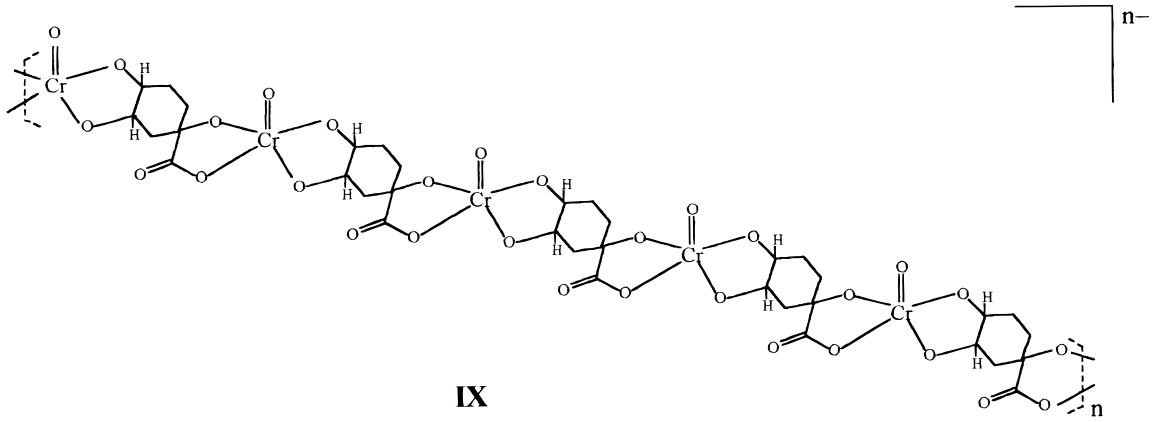

IX

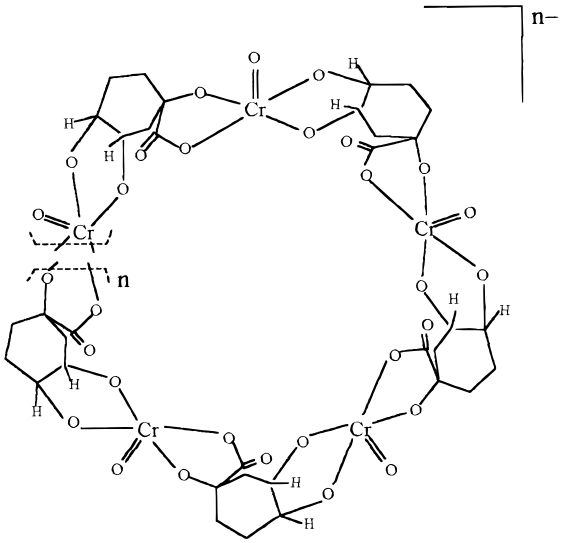

X

ever, such linkage isomerism for $K[Cr(O)(qaH_3)_2]\cdot H_2O$ at pH < 5.0 is not consistent with the experimental results, which would result in a pH dependence of the ratio of signals due to different degrees of ligand deprotonation in the linkage isomers. Therefore, the two signals at these low pH values must be due to geometric isomers. The relative concentrations of the geometric isomers of $Na[Cr(O)(hmba)_2]\cdot H_2O$ were estimated from the relative ratios of the high field ^{53}Cr-hyperfine satellite signals as 70:30 ($A_{iso} = 17.4 \times 10^{-4}$ cm^{-1}: $A_{iso} = 16.3 \times 10^{-4}$ cm^{-1}). The simulation of the central signal of the EPR spectrum of $Na[Cr(O)(hmba)_2]\cdot H_2O$, using this ratio as a guide, "resolves" the broad central signal into two species with $g_{iso} = 1.9784$ ($A_{iso} = 17.4 \times 10^{-4}$ cm^{-1}) and $g_{iso} = 1.9786$ ($A_{iso} = 16.3 \times 10^{-4}$ cm^{-1}). Therefore, in the case of $K[Cr(O)(qaH_3)_2]\cdot H_2O$, the g_{iso} values are separated by 0.0004 units compared to 0.0002 units for $Na[Cr(O)(hmba)_2]\cdot H_2O$. In the latter case, the separation of the g_{iso} values of the species is insufficient to effect unambiguous resolution of the central EPR signal. This may be due to exchange broadening, and detailed studies at higher frequency (Q-band) would be required to establish whether the differences in g_{iso} values have a kinetic or thermodynamic origin. The similarity in results obtained by the reduction of Cr(VI) by GSH in the presence of qaH_5 and the spectra of $[Cr(O)(qaH_3)_2]^-$ at low pH values shows that qaH_5 is an effective competitor for Cr(V), since Cr(V)-GSH complexes give distinct EPR signals ($g_{iso} = 1.996$, $g_{iso} = 1.986$).[11] The temperature dependence of the geometric isomers of $[Cr(O)(qaH_3)_2]^-$ is similar to those of V(IV)-lactic or glycolic acid complexes. At near neutral pH values, two signals were observed in the EPR spectrum of an aqueous solution of V(IV) and lactic acid, which were found to be independent of the pH value and both the ligand and V(IV) concentrations.[60] The ratio was found to vary, however, as a function of temperature. The study concluded that the most likely explanation for the two species was the presence of two geometric isomers.[60] There are parallels between the V(IV)-lactic acid study and the current work in that the species with the higher g_{iso} value has the lower A_{iso} value. The similar trends in temperature dependence that exist between two systems, where in one case ((V(IV)-lactic acid) no linkage isomerism is possible, are consistent with other evidence for geometric isomerization.

At higher pH values (>5), new signals appear with ^{1}H a_{iso} values ranging between 0.80×10^{-4} and 0.95×10^{-4} cm^{-1}, which is in good agreement with the ^{1}H a_{iso} values observed in the EPR spectra of complexes formed between Cr(V) and adenosine (0.75×10^{-4} cm^{-1})[38] or rhamnose (0.84×10^{-4} cm^{-1}),[47] where complexation occurs via the *cis*-diol group of the sugar. Additional evidence in support of the linkage isomerism processes is the pH dependence of the equilibria and the similarity of the spectra of the high g_{iso} value signals for

(60) Reeder, R. R.; Rieger, P. H. *Inorg. Chem.* **1971**, *10*, 1258−1264.

qaH_5 and the species generated for saH_4, which can only form 1,2-diolato complexes.

Linkage Isomerism in $[Cr(O)(saH)_2]^{3-}$. The g_{iso} and A_{iso} values of the saH_4 complexes are typical of five-coordinate oxo-Cr(V) species with four alcoholato donors.[41] This ligand can form three linkage isomers with Cr(V), by virtue of the two pairs of *vic*-diol groups (**XI**−**XIII**). Since the ^1H a_{iso} value is

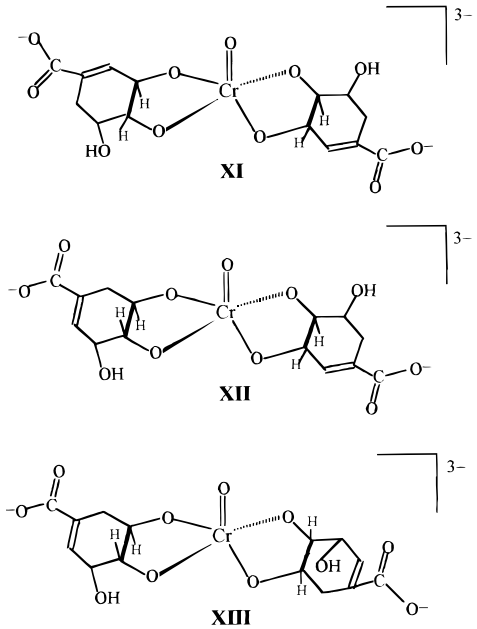

similar to that observed for the bis-chelate species formed between Cr(V) and *cis*-1,2-cyclohexanediol,[37] the dominant Cr(V)-sa linkage isomer is also likely to feature *cis*-diol (3,4-) coordination (**XI**). The dominance of $[Cr(O)(O^3,O^4\text{-}saH)_2]^{3-}$ is an excellent example of the preference for Cr(V) to bind to *cis*- rather than *trans*-diol groups. This has been illustrated previously on several occasions for Cr(V),[43,46] and also for V(IV)-diol binding.[59] Binding via the 4,5-diol group is evident in Cr(V)-qa species, which indicates that the donor properties of the 3,4-diol in saH_4 may be either sterically or electronically enhanced, compared to qaH_5.

Cis vs Trans Binding in Cr(V)-Diol Complexes and Deconvolution of EPR Spectra. In the Cr(V)-qa system, the concentration of **IV** would be expected to be greater than that of **V**, based on the intramolecular competition experiments using saH_4, which established a clear preference for *cis*- rather than *trans*-diol binding to Cr(V). This is borne out by the equilibrium constant for the formation of **IV** being 10 times the value for **V**. The equilibrium constant for the formation of the bis-chelate complex formed between V(V) and *cis*-1,2-cyclohexanediol is also 10 times greater than that for the *trans*-analogue.[61] The marked dominance of the binding of Cr(V) to *cis*- rather than *trans*-diol groups is easily rationalized, since the torsion angle of the chelate ring (O−C−C−O) in a *cis*-geometry can accommodate a reduction in the angle size ($\leq 60°$), which facilitates coordination. The same angle in a *trans*-diol arrangement cannot be less than 60°. This affect has been described in relation to the coordination of the isoelectronic V(IV) ion with sugars.[59] The linkage isomers, **IV**, **V**, and **VI**, would be predicted to yield a doublet, a singlet, and a triplet, respectively, where the EPR spectral multiplicity is a function of the number and orientation (cis- or trans-) of the ring protons of the coordinated diol group. In accordance with the preference shown by Cr(V) toward *cis*- rather than *trans*-diol binding, the concentration of the alternative bis-diol linkage isomers, **VII** and **VIII**, would be expected to be small, compared to **VI**. The presence of **VII** or **VIII** is not required to obtain a good fit between the observed and simulated EPR spectra.

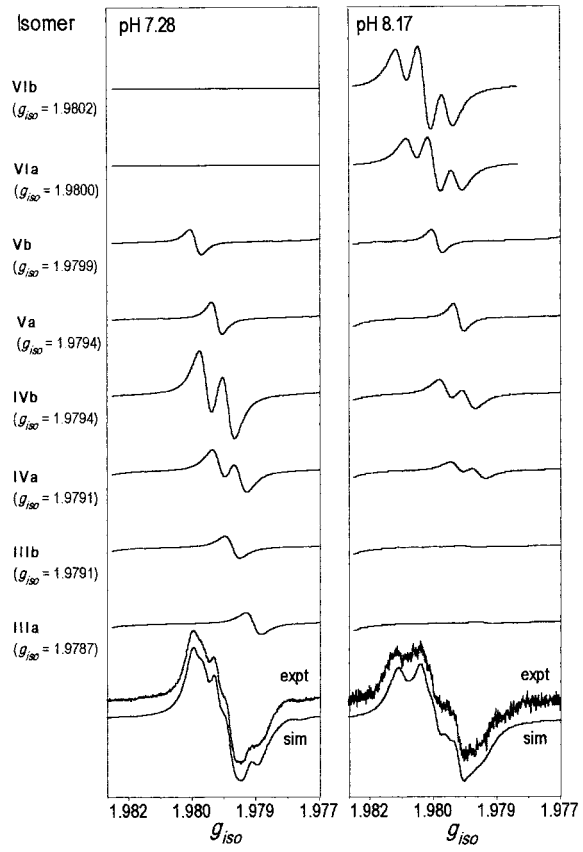

Figure 7. Predicted EPR spectra and relative concentrations of the individual Cr(V) linkage (**III**−**VI**) and geometric (a, b) isomers postulated to form in the reduction of Cr(VI) (40 mM) by GSH (2 mM) in the presence of qaH_5 (100 mM) at pH 7.28 and 8.17. The lowest graphic shows the spectrum of the sum of all the predicted spectra for the individual species (sim) and the experimentally observed spectrum (expt).

At pH values between 5.0 and 8.0, the predominant Cr(V)-qa linkage isomers feature mixed-binding modes, with 2-hydroxy acid and diol donors. The Cr(V)-qa EPR spectra have been deconvoluted into the spectra predicted for the individual linkage isomers (Figure 7). Notably, the g_{iso} values of the purported geometric isomers of **XI** differ only by 0.0001 units. The differences in the g_{iso} values (Δg_{iso}) of the purported geometric isomers for each Cr(V)-qa linkage isomer were 0.0004 for **III**, 0.0003 for **IV**, and 0.0005 for **V**. These differences in g_{iso} values are more significant than that noted for the geometric isomers of **VI** (0.0002). This indicates that the changes to the electronic structure of geometric isomers of Cr(V) complexes with mixed-donor types (i.e., bis-(2-hydroxy acid), 2-hydroxy acid-diol) are greater than for the case where the donor types are similar (i.e., bis-diol).

Minor Species at Low g_{iso} Values. The formation of the additional signal at g_{iso} ~1.9792 in the Cr(VI)/GSH/saH_4 reaction is pH-dependent, as opposed to the formation of the bis-diol Cr(V)-sa species, which is invariant of pH (at pH values >5.5). The g_{iso} value is too high to support the presence of six-coordinate oxo-Cr(V) complexes.[41] The signal is broad, with a discernible shoulder, which was simulated as having ^1H-superhyperfine coupling arising from diol coordination. An oxo-

(61) Tracey, A. S.; Gresser, M. J. *Inorg. Chem.* **1988**, *27*, 2695−2702.

Cr(V) complex featuring one diol group and two monodentate carboxylato donors, $[Cr(O)(O^7\text{-}saH_3)_2(O^3,O^4\text{-}saH)]^{2-}$ (**XIV**), is consistent with the dependence (relative to the bis complexes) of the signal on both pH (at pH values <4.01) and ligand concentration (at pH values ~3.8). Monodentate carboxylato coordination has been observed previously in species formed between Cr(V) and acetic acid.[62,63] It should be noted that the formation of **XIV** from **XI** is dependent upon the pK_a value of saH_4. If saH_4 was deprotonated (i.e., at pH values >4.01),[55] an alternative structure **XV** would also be consistent with the ligand

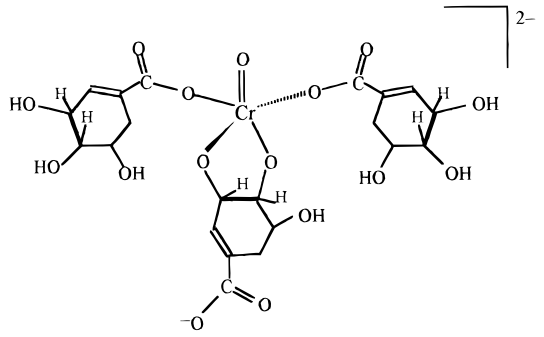

XIV

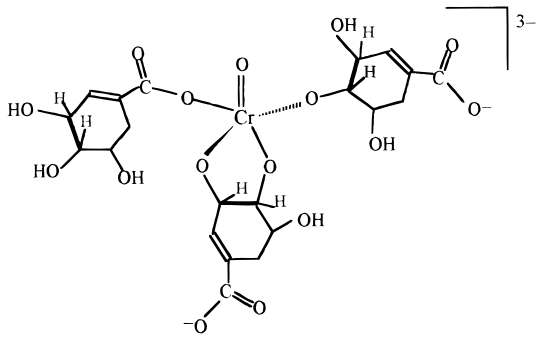

XV

concentration dependence data. The latter structure gives good agreement between the observed and calculated[41] g_{iso} values (1.9792 and 1.9791, respectively). The formation of **XV**, however, would be independent of pH (at pH values < pK_a value of saH_4), which is not the case here.

The minor signals produced upon the reduction of Cr(VI) by GSH in the presence of excess qaH_5 at high pH values (pH 6.18 and 6.91) are not observed in the Cr(VI)/GSH/saH_4 reaction. Therefore, it is unlikely that the species solely feature ancillary donors, such as aqua or hydroxo groups. Similar signals were observed in Cr(V)-D-glucose studies and were attributed to Cr(V) species formed with glucose oxidation products.[37] It is possible that the minor Cr(V)-qa species contain oxidized ligand, since the same oxidation of saH_4 at C(1) is not possible due to the unsaturation in the cyclohexane ring. Coordination to oxidized ligand, however, is inconsistent with the fact that Cr(VI) is a stronger oxidant at acidic pH values.[24] The relative concentrations of these minor signals are independent of ligand concentration, which is consistent with the responsible species being a bis-chelate, but the low g_{iso} values of the species suggest the presence of six-coordinate oxo-Cr(V) species.[41] Possible six-coordinate species may feature triol binding via either the 1,3,4- (**XVI**), 1,3,5- (**XVII**), or 1,4,5- (**XVIII**) triol groups. These binding modes would not be observed between Cr(V) and saH_4, since the ligand does not have a 1-OH group. The calculated g_{iso} value for a six-coordinate oxo-Cr(V) species with five alcoholato donors (g_{iso} = 1.9759) is in reasonable agreement with the observed g_{iso} values. The high negative charges of these species are also consistent with their appearance at high pH values.

The possibility of 3,4,5-triol binding is unlikely because the model of this structure is quite strained.[64] Also, the signals at low g_{iso} values are not observed in the saH_4 system, in which the 3,4,5-triol coordination mode is also possible. On the basis of molecular models, the 1,3,4-triol bound Cr(V)-qa complex (**XVI**) is the least strained.[64] The ligand in this structure is in a half-boat conformation and has one five-membered and one six-membered chelate ring. Although in the 1,3,5-triol Cr(V) complex (**XVII**) the ligand remains in the energetically favored conformation, the structure is somewhat strained, most probably due to the presence of two six-membered chelate rings. Of the three structures, **XVIII** is the most strained and is quite unlikely to be formed in significant amounts.

^{1}H-Superhyperfine Coupling. The lack of structural data for Cr(V)-diol complexes can be addressed by examining analogous structures formed between V(V) and cyclic diols. Recently, the structures of two V(V) complexes with *sec*-*cis*-diol ligands have been solved by X-ray crystallography.[65,66] The complexes formed between V(V) and either methyl-*O*-4,6-benzylidene-α-D-mannopyranoside (MBMP)[65] or adenosine[66] are dinuclear, with the V(V) ions bridged by an alcoholato donor from the sugar ring. Complexes between V(V) and the 2-hydroxy acids, $hmbaH_2$ and $ehbaH_2$, also have this structural motif.[67,68] The distorted-TBP coordination sphere of V(V)-ehba and -hmba dinuclear complexes is similar to that of the mononuclear Cr(V) complexes with the same ligands.[28,69] Therefore, it is reasonable to assume that complexes formed between either V(V) or Cr(V) and cyclic diols would have similar structures. Two analyses have been used to assess the spatial relationship between the ring protons of the coordinated diol groups and the V(V) nuclei. First, the distance between the proton and the ligand plane has been determined, where the ligand plane is defined as the plane containing the donating diol O atoms (2), the second-shell C atoms (2), and the V(V) atom. Second, the dihedral angle, H−C−O−V, has been calculated. These results (Table S2; refer to V(V) and Cu(II) structures for clarification of the atom labeling schemes) show that, in complexes formed between V(V) and *cis*-cyclic diols, one proton essentially lies in the ligand plane, while the other proton lies perpendicular to the ligand plane. Therefore, the two protons of *cis*-cyclic diols are oriented quite differently with respect to the metal ion and would experience different degrees of orbital overlap with the metal orbital containing the unpaired electron. In the case of *trans*-diol binding, the ring-protons lie above and below the ligand plane, resulting in limited overlap. This scenario is well illustrated by the X-ray crystal structure of the polymeric complex formed between Cu(II) and qaH, in which the ligand is coordinated via the 2-hydroxy acid (O^1,O^7)

(62) Kon, H. *J. Inorg. Nucl. Chem.* **1963**, *25*, 933−944.
(63) Farrell, R. P., Ph.D. Thesis, The University of Sydney, 1993.
(64) *Cochranes of Oxford Molecular Models: Orbit System and Minit System*; Oxford, U.K., 1973.
(65) Zhang, B.; Zhang, S.; Wang, K. *J. Chem. Soc., Dalton Trans.* **1996**, 3257−3263.
(66) Angus-Dunne, S. J.; Batchelor, R. J.; Tracey, A. S.; Einstein, F. W. B. *J. Am. Chem. Soc.* **1995**, *117*, 5292−5296.
(67) Judd, R. J., Ph.D. Thesis, The University of Sydney, 1992.
(68) Hambley, T. W.; Judd, R. J.; Lay, P. A. *Inorg. Chem.* **1992**, *31*, 343−345.
(69) Judd, R. J.; Hambley, T. W.; Lay, P. A. *J. Chem. Soc., Dalton Trans.* **1989**, 2205−2210.

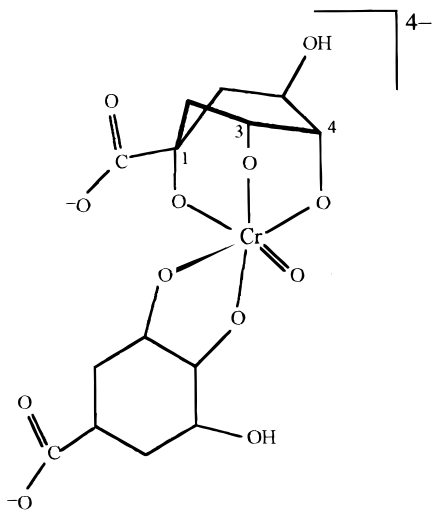

XVI

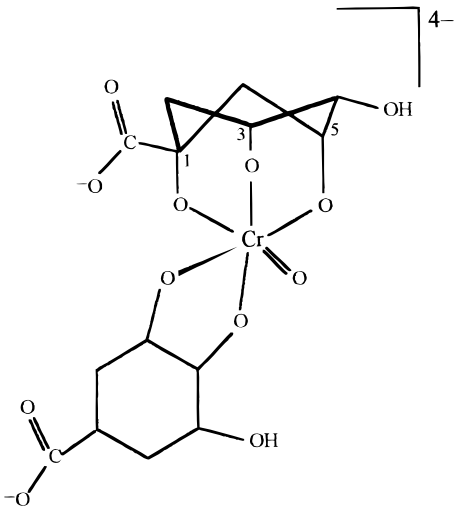

XVII

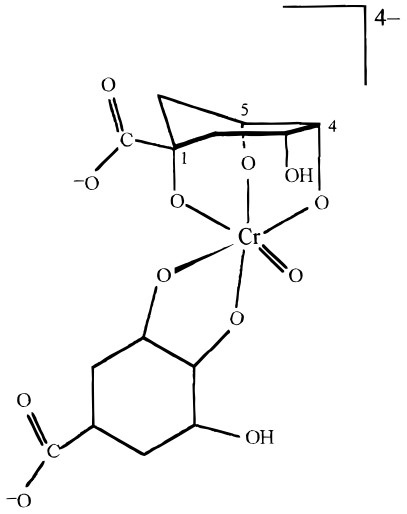

XVIII

and the *trans*-diol (O^4,O^5) region.[70] As predicted, the ring protons lie well above [H(5i)] and below [H(4i)] the ligand plane, which is similarly reflected in the dihedral H−C−O−Cu angles (Table S2). Recent studies of the EPR spectra of species formed between Cr(V) and cis- or *trans*-1,2-cyclohexanediol have shown that the proton lying in the ligand plane couples to a greater extent with the unpaired electron on the Cr(V) ion, compared to the proton lying perpendicular to the ligand plane.[37] This seems reasonable since the overlap between the proton *s* orbital and the Cr(V) orbitals containing the unpaired electron density will be maximized when the H−C−O−Cr dihedral angle is closer to 0°, as in *cis*-cyclic diols, compared to *trans*-cyclic diols, where the same angle approaches 90° (Table S2). It is for these reasons that the EPR spectrum of the species formed between Cr(V) and saH_4 yields a triplet rather than a quintet, since only one proton per ligand is in the plane of the unpaired electron density of the Cr(V) ion. In contrast to cyclic-diol ligands, the protons of linear diols are magnetically equivalent due to rapid Berry twists, and therefore, the spectral multiplicity is a function of the number of protons and the rate of the fluxional behavior,[35,36] as revealed from ENDOR spectroscopic studies at low temperature.[34]

Conclusions

There is no doubt that small-molecule reductants, such as ascorbate and GSH, play an important role in intracellular Cr(VI) metabolism.[71,72] What has been over-looked, perhaps due to the unfavorable kinetics of Cr(VI) reduction by alkoxide-containing molecules,[24] is the importance of Cr(V)-diol species with respect to Cr(VI) metabolism. The results obtained here clearly establish that the reduction of Cr(VI) by GSH, in the presence of an excess of diol-containing ligands, yield long-lived EPR-active Cr(V)-diol species at physiological pH values. The nature of the Cr(V)-diol species found here is also consistent with those observed in the ligand-exchange reaction between $Na[Cr(O)(ehba)_2]\cdot H_2O$ and D-glucose,[37] where there is a marked

(70) Bkouche-Waksman, I. *Acta Crystallogr., Sect. C* **1994**, *50*, 62−64.

(71) Standeven, A. M.; Wetterhahn, K. E. *Carcinogenesis* **1992**, *13*, 1319−1324.

(72) Zhang, L.; Lay, P. A. *J. Am. Chem. Soc.* **1996**, *118*, 12624−12637.

preference for coordination to donors disposed in a cis rather than a trans fashion. At pH values <4, the 2-hydroxy acid mode of binding between Cr(V) and qaH_5 predominates, which has relevance in terms of the local acidic cellular environment following phagocytosis. During phagocytosis, the vesicles experience a drastic decrease in pH. Over a 20 min period, for example, the pH value of a phagocytic cell dropped from 6.70 (t = 2 min) to <5 (t = 22.5 min).[48] This has important implications with respect to the cellular uptake of water-insoluble carcinogens and has particular relevance to intracellular Cr(VI) metabolism on two accounts.[73] First, the redox potential of Cr(VI) is higher at acidic pH values than at neutral pH. Second, Cr(V)-2-hydroxy acid complexes, which have been implicated as possible intermediates in Cr(VI)-induced carcinogenesis, are considerably more stable in this pH region, compared to near neutral pH values.[51] By contrast, the diol-binding mode is preferred at normal physiological pH values (~7.4) relevant to the intra- and intercellular environments encountered by soluble Cr(VI) compounds. The Cr(V)-diol species are remarkably stable, with increases in the EPR signal (at pH 6.91) observed at 1 h after the initiation of the reaction (data not shown). The relevance of Cr(V)-diol complexes with respect to Cr(VI) metabolism is highlighted by the results of a recent in vivo EPR study of the Cr(V) species formed in rats,[40] where the EPR signals have g_{iso} and ^1H a_{iso} values very similar to those of the species described in the current work and are likely to be bis-chelate Cr(V)-diol complexes. It is becoming more apparent that diol ligands play an important role in the stabilization of Cr(V) species. It may be more appropriate to think of the small-molecule Cr(VI) reducing agents, such as GSH and ascorbate, as detoxifying agents, where the ultimate genotoxic agents are species formed between Cr(V) and sugars or sugar-like molecules. Indeed, ascorbate has been used as a Cr(VI)-detoxifying agent in skin preparations (1% ascorbic acid in poly(ethylene glycol)) for sufferers of Cr(VI)-induced dermatitis and in the protective masks of workers exposed to chromic acid mists.[24]

(73) Farrell, R. P.; Costa, M. In *Comprehensive Toxicology*; Sipes, I. G., McQueen, C. A., Gandolfi, A. J., Eds.; Pergamon Press: New York, 1997; Vol. 12, p 225−253.

Acknowledgment. The authors are grateful for an Australian Postgraduate Research Scholarship (R.C.) and an Australian Research Council (ARC) Grant (P.A.L.) and ARC RIEFP Grants for EPR and CD spectrometers. We thank the Australian National University Microanalytical Service for microanalyses (C, H, and Cr).

Supporting Information Available: Values of K_1, for the Cr(VI)/GSH/saH_4 reaction and of selected molecular geometry parameters of V(V)- or Cu(II)-cyclic diol complexes (with structures) are presented in Table S1 and Table S2, respectively. The EPR spectra of the Cr(VI)/GSH/qaH_5 reaction as a function of [qaH_5] at pH 4.0 (Figure S1), at pH 6.4 (Figure S3), and at pH 4.0, where [qaH_5]/[Cr(V)] is constant (Figure S2), are included. The plot of ln K vs 1/T for the aqueous speciation of $[Cr(O)(qaH_3)_2]^-$ is given in Figure S4. The ^{53}Cr hyperfine signals in the Cr(VI)/GSH/saH_4 reaction (pH 6.84) or the Cr(VI)/GSH/qaH_5 reaction (pH 4.17 and 6.18) are given in Figures S5 and S8, respectively. The EPR spectra of the [saH_4] dependence of the Cr(VI)/GSH/saH_4 reaction (pH 6.80) and the plot of [B]/([A][H^+]) vs [saH_4] (pH 3.0) are given in Figures S6 and S7, respectively. The plot of [D]/[C] vs 1/[H^+] for the Cr(VI)/GSH/qaH_5 reaction is given in Figure S9. The EPR spectra of the Cr(V) intermediates in the Cr(VI)/GSH/qaH_5 reaction with increasing [qaH_5][Cr(VI)] at pH 6.90 are presented in Figure S10. This material is available free of charge via the Internet at http://pubs.acs.org.

JA9909780